Bulgarian Chemical Communications, Volume 48, Number3 (pp. 565 – 570) 2016

Synthesis, structural and biological studies of cobalt ferrite nanoparticles

M.W. Mushtaq[1], M. Imran[1], S. Bashir[2], F. Kanwal[1], L. Mitu[3*]

[1]Institute of Chemistry, University of the Punjab, Lahore-54890, Pakistan
[2]Centre of Ionics, Department of Physics, Faculty of Science, University of Malaya-50603, Kuala Lumpur, Malaysia
[3]Department of Chemistry, University of Pitesti, Pitesti-110040, Romania

Received May 31, 2015; Accepted December 16, 2015

Cobalt ferrite's nanoparticles, $CoFe_2O_4$ (CF) were synthesized via the co-precipitation method using a new monomeric surfactant called sorbitol. Fourier Transform Infrared (FTIR) spectroscopy, X-ray powder Diffraction (XRD), a Vibrating Sample Magnetometer (VSM) and Scanning Electron Microscope (SEM) were used for their characterization. The presence of an (M–O) bond was confirmed by the absorption band at 589 cm^{-1} in the FTIR spectrum. VSM studies revealed the super paramagnetic nature of cobalt ferrite nanoparticles having a saturation magnetization value of 62.55 emu/g and 59.89 emu/g for cobalt ferrite NPs prepared without and with surfactant assistance respectively. The hysteresis loops showed negligible hysteresis, remanence and coercivity at 300 K. The powder X-ray Diffraction (XRD) pattern confirmed a single phase spinel cubic structure. SEM micrographs have been used to confirm the particle size which is found to be 28 nm with the surfactant and 60 nm without the surfactant and to analyse the distribution of NPs. Thermogravimetric measurements have also been studied to measure the presence of surfactant. The synthesized nanoparticles via the surfactant method were screened for their antibacterial activity against Escherichia Coli and Staphylococcus Aureus and demonstrated an appreciable activity. Furthermore, the interaction of cobalt ferrite nanoparticles with calf-thymus DNA was also investigated.

Keywords: Cobalt ferrite, Nanoparticles, Antibacterial activity, Calf-thymus DNA.

INTRODUCTION

In the past decade, nano-sized ferrite particles gained an attraction as a new emerging class of inorganic compounds because of their comprehensive applications in applied chemistry, high-density data storage, biochemistry, MRI and targeted drug delivery [1-3]. The paramount features about ferrite nanoparticles (NPs) established in the literature are that these compounds are non-toxic, biofriendly and exhibit strong antibacterial potential and magnetic capability [4,5]. Among these compounds, some notable examples of ferrites are iron Oxide (Fe_3O_4), nickel ferrite ($NiFe_2O_4$), manganese ferrite ($MnFe_2O_4$) and cobalt ferrite ($CoFe_2O_4$) nanoparticles that possess biocompatibility, small size, minimum toxicity and superparamagnetic properties enabling them as suitable candidates in the biomedical sciences. Ferrites are a family of metal oxides having a spinel structure MFe_2O_4 (M = Fe^{+2}, Co^{+2}, Ni^{+2}, Zn^{+2}, Mg^{+2}, etc.). The distribution of metal ions in ferrite NPs $[M^{+2}]_{tetra}[Fe^{+3}]_{octa.}O_4$, modifies their magnetic behaviour.

One of the important type of nanoferrites is cobalt ferrite (CF) which exhibits an inverse spinel structure, a high curie temperature, superior chemical and mechanical stability and a large magnetic spin magnitude [6,7]. Cobalt ferrites ($CoFe_2O_4$) NPs have been synthesized by various physico-chemical methods such as hydrothermal reaction, micro-emulsion, sol-gel and co-precipitation techniques [8-10]. Relative co-precipitation is found to be the most used [11]. It is established in the literature that the nanostructure of cobalt ferrite possess Co^{+2} ions in octahedral sites (B) while Fe^{+3} ions are equally distributed between tetrahedral (A) and octahedral sites (B) [12].

To apply ferrite NPs in the engineering and biomedical fields, it is crucial to control the size, morphology and surface properties. During the genesis and growth of the primary nanoparticles, the surface chemistry of the primary nanoparticles is an important factor to control the final structure of the secondary nanoparticles by a process called Ostwald ripening, aggregation and coarsening [13]. The introduction of surfactants as a capping agent during synthesis of NPs, has been widely applied to control the size as well as the mechanical stability of ferrites as reported in the literature [14]. Various capping agents were applied to control the growth of building blocks of NPs including monomeric surfactants (ethylene glycol, glycerol, etc.)[15] and polymeric surfactants (PEG_{300}, PEG_{600}, PEG_{1000},

* To whom all correspondence should be sent:
E-mail: ktm7ro@yahoo.com

PEG_{10000}, PVP_{40000}, etc.)[16]. However, post treatment of NPs with monomeric surfactant is more beneficial because the polymeric surfactant may decrease the surface area by increasing the particle size. With monomeric surfactant, the particle size of the ferrites is easily controllable and a uniform distribution of metal ions is observed in octahedral and tetrahedral sites.

Keeping in view the literature and interesting features of cobalt ferrite nanoparticles, we have synthesized them by using a wet chemical route following the addition of a novel monomeric surfactant called sorbitol to explore their characteristic aspects as well as their biological properties.

EXPERIMENTAL

Materials: Iron chloride $FeCl_3{\cdot}6H_2O$ (98%), cobalt chloride $CoCl_2{\cdot}6H_2O$ (98%) were purchased from Uni-chem. Sodium hydroxide (99%) was procured from Riedel-de Haen while sorbitol and calf thymus DNA from BDH-England and Sigma Aldrich respectively. All these purchased chemicals were used without further purification.

The preparation of cobalt ferrite ($CoFe_2O_4$) nanoparticles: $FeCl_3{\cdot}6H_2O$ (0.03 mol, 8.109 g) and $CoCl_2{\cdot}6H_2O$ (0.015 mol, 3.567 g) were dissolved together in 100ml of double de-ionized water. Then sodium hydroxide solution (0.3 mol, 12g/100 ml) was added slowly until a pH of 11−12 was reached. The resulting reaction mixture was subsequently stirred at 80°C for 1h. Upon stirring a black coloured precipitate started to settle down. Finally, the formed precipitates were cooled, filtered, washed with de-ionized water and then by ethanol. The resulting solid was then dried at 100°C for 1h [17]. We also synthesized $CoFe_2O_4$ NPs by adding 2-3 drops of sorbitol (0.01 mol, 1.82 g) as a monomeric surfactant or capping agent while keeping all other parameters constant as mentioned above. The corresponding nanopowders obtained without and with a surfactant assisted approach are called product a and b respectively.

Characterization: Powder X-ray diffraction (PXRD) analysis was conducted on a Philips analytical X-ray diffractometer using CuKα radiation (λ = 0.154 nm). Fourier transform infrared (FTIR) absorption spectra were recorded using a Cary 630 FTIR spectrometer in the wave number range of 4000−400 cm^{-1} with potassium bromide (KBr) pellets. UV–Vis spectra of pure cobalt ferrite NPs were obtained by using a UV–Vis spectrophotometer (UV-2600, Shimadzu). The magnetic behavior was studied by using a Lakeshore-7404 vibrating sample magnetometer (VSM) at room temperature, 27°C up to a maximum applied magnetic field of 10 KOe.

Biological Studies

Antimicrobial studies; $CoFe_2O_4$ were screened for their antibacterial potential against Staphylococcus aureus and Escherichia coli strains by the Kirby-Bauer technique [18]. The antibacterial actvity was determined by measuring the clear zone of inhibition after incubation for 24 h at 37°C.

Interaction between DNA and cobalt ferrite nanoparticles; the nanocomposite DNA/$CoFe_2O_4$ was prepared by mixing 0.1 mg/ml of calf-thymus DNA (0.308 mM for the Phosphate group) and 0.5 mg/ml of cobalt ferrite NPs in a Tris-Hcl buffer (10 mM, pH = 7.5). The resulting bionanocomposite was isolated from the solution using magnetic separation and washed with double distilled water. The concentration of DNA was recorded by a UV-Vis Spectrophotometer at 260 nm. The amount of adsorbed DNA was calculated by the following formula:

$$A = [(Co - Ci)v/m] \times 100\%$$

where Co is the initial concentration (mg/ml) of DNA in the solution, Ci is the concentration (mg/ml) of unbounded DNA molecules, V is the volume of the reaction medium in ml and m is the mass of CF nanopowder. The adsorption capacity was expressed in mol/g and mol/m^2 taking into account that 1 mg/ml of DNA concentration corresponded to a 3.08 mmol/l concentration of the DNA phosphate group.

RESULTS AND DISCUSSION

The UV-Visible spectrum of $CoFe_2O_4$ NPs synthesized by the surfactant assisted method is shown in Fig.(1). It displays a characteristic band in the range 330−450 nm, which developed particularly from the dispersion and absorption phenomenon of $CoFe_2O_4$ magnetic nanoparticles and is in agreement with previous relations [18].

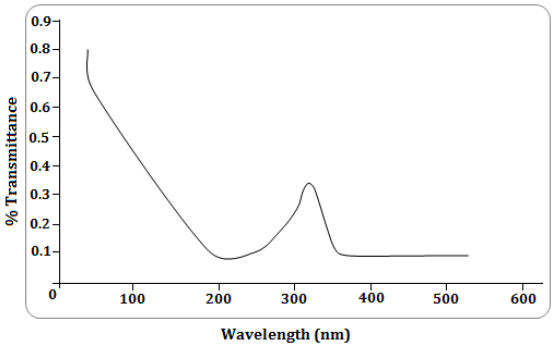

Fig. 1. UV-Visible spectrum of cobalt ferrite NPs.

Fig. 2 shows the effect of an applied magnetic field on the magnetization (emu/g) value of prepared cobalt ferrite NPs without and with the assistance of surfactant called product a and b respectively at room temperature. The M−H curves of both products (a, b) indicate types of hysteresis loop formation for soft magnetic materials with negligible coercivity, Hc∼17.62 and ∼16.94. It was also observed that by increasing the strength of the applied field, the value of saturation magnetization (Ms) for product a and b sharply increases and becomes nearly saturated at about 62.55 (emu/g) and 59.89 (emu/g) respectively, suggesting the presence of small magnetic particles exhibiting superparamagnetic behaviour of CF nanoparticles [18]. Fig.(2b) affirms that the magnetic feedback is not significantly altered by applying a sorbitol coating as a surfactant on the cobalt ferrite nanoparticles. However, the small decrease in the Ms value of the surfactant assisted prepared cobalt ferrite NPs is due to the small size of the magnetic core than the uncoated cobalt ferrite NPs. In addition to this, the non-magnetic coating layer of sorbitol can behave as a magnetic dead layer on the surface of cobalt ferrite NPs, thus reducing their saturation magnetization potential [19].

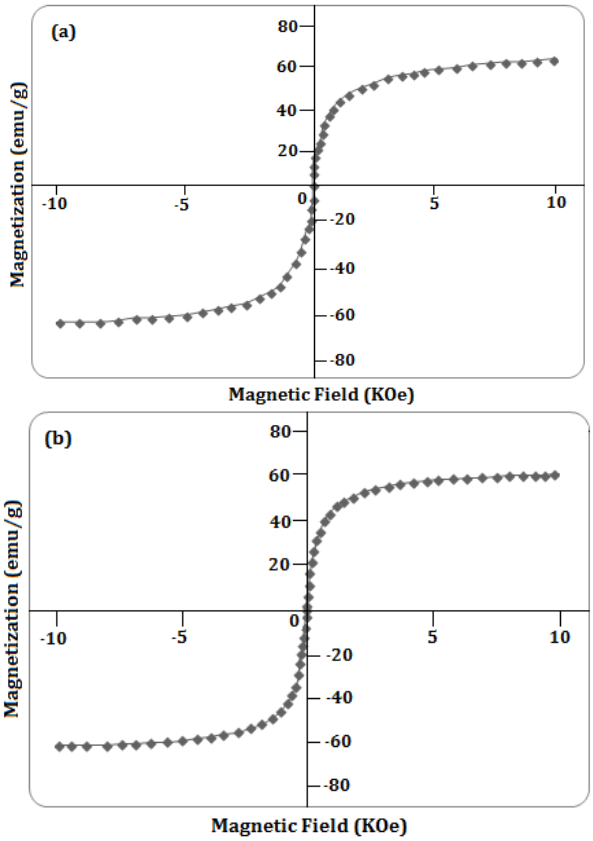

Fig. 2. (a) Effect of an applied field on the magnetization value of cobalt ferrite NPs prepared without surfactant (b) with surfactant.

FT-IR spectra of pure cobalt ferrite NPs synthesized without and with the sorbitol assisted method at room temperature are shown in Fig.(3). Two characteristic bands at ∼598, ∼592 and ∼492, ∼484 cm^{-1} were observed in both products a and b which may correspnd to intrinsic stretching vibrations of the metal at a tetrahedral site (M_{tetra}–O) bond and at an octahedral site (M_{octa}–O) respectively [20,21]. The other important peaks of products a and b at ∼3440, ∼3478 and ∼1640, ∼1636 cm^{-1} can be attributed to H−O−H stretching and bending vibrations of the absorbed water molecules on the surface of cobalt ferrite NPs respectively [22]. The additional peaks observed in Fig.(3b) at 2930 and 2864 cm^{-1} correspond to υ_{as}(C−H) and υ_{s}(C−H) respectively and confirm the coated layer of sorbitol surfactant.

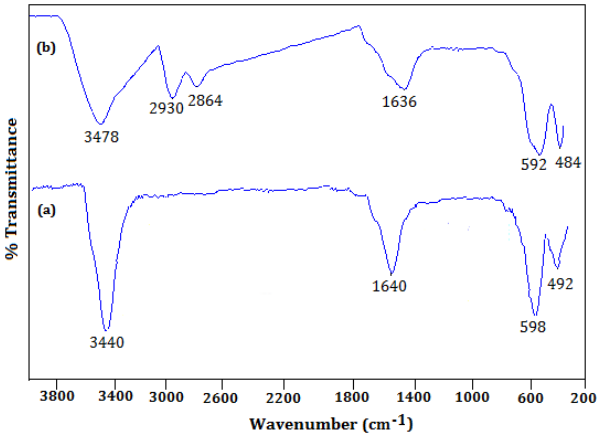

Fig. 3. (a) FT-IR spectra of $CoFe_2O_4$ nanoparticles synthesized without surfactant (b) with surfactant assistance.

DSC/TGA was carried out in the temperature range 25°C to 650°C and the curves of the product b prepared with surfactant are shown in Fig.(4). The TGA curve in Fig.(4) exhibits two steps attributed to individual weight loss. The first loss was observed in the range 25°C to 150°C while the second loss appeared in the range 300°C to 450°C. The DSC curve shows a broad endothermic peak at 150°C. This might be due to desorption of water molecules from the surface of the surfactant and cobalt ferrite. The exothermic peak in the DSC curve was observed at 350°C. The exothermic peak can be reffered to the combustion of coated surfactant. Above 450°C, no weight loss was found indicating the presence of only cobalt ferrite nanoparticles in the temperature range 450°C to 650°C [23,24].

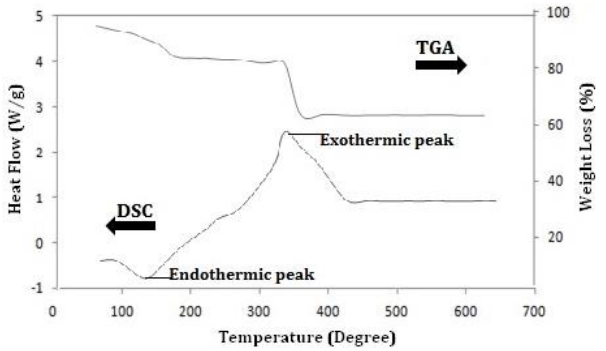

Fig. 4. DSC/TGA curves of cobalt ferrite nanopowder.

The X-ray diffraction pattern of $CoFe_2O_4$ nanoparticles prepared in the form of product a and b is presented in Fig.(5). All the characteristic peaks in both products at angles 18.29°, 30.08°, 35.44°, 37.06°, 43.06°, 53.45°, 56.98° and 62.59° are indexed as the reflection planes of (111), (220), (311), (222), (400), (422), (511) and (440) respectively. These peaks exactly match the JCPDS (22-1086) data and confirm the single phase inverse spinel structure of the $CoFe_2O_4$ nanocrystals [25,26]. However, product a shows an improvement of the crystalline phase of cobalt ferrite NPs as compared to product b which was prepared in the presence of the surfactant. The particle size has been determined by the Debye Sherrer equation ($D = 0.9\lambda/\beta\cos\theta$, where D is the crystalline size, λ is the wavelength of the X rays, β is the full width at half maximum of the diffraction peak and θ is Bragg's angle) which is 65 nm and 32 nm for product a and b respectively. In product b the presence of a broad diffraction plane (311) justifys the smaller $CoFe_2O_4$ NPs formed in the presence of a capping agent. This fact may be due to the performance of a monomeric surfactant in the reduction of clustering of the nanoparticles[15].

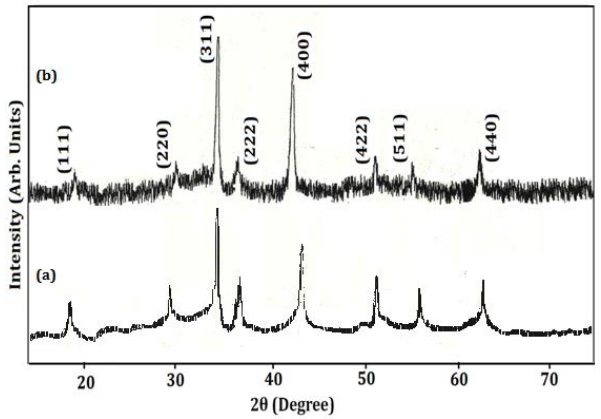

Fig. 5. X-ray diffraction pattern of $CoFe_2O_4$ nanoparticles prepared (a) without a surfactant (b) with an additional surfactant.

SEM analysis of the cobalt ferrite NPs prepared without and with a surfactant are shown in Fig.(6). The average size of the cobalt ferrite NPs was about 60 nm and 28 nm for products a and b respectively which nearly matches the crystallite sizes calculated by XRD. The morphology of the cobalt ferrite NPs in product a is comprised of spherical nanocrystallites and has a uniform distribution of nanoparticles which defines the effectiveness of the surfactant. However, a slight compactness and clustering of NPs were observed in the case of product b.

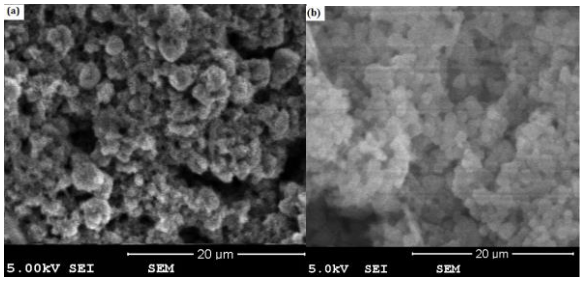

Fig. 6. (a) SEM images of Cobalt ferrite NPs prepared without a surfactant (b) with a surfactant.

The antibacterial potential of $CoFe_2O_4$ NPs prepared by the surfactant method (product b) was screened against two common bacterial pathogens, *Escherichia coli* and *Staphylococcus aureus.* Generally, it was found that Gram negative strain *E.coli* is more sensitive to $CoFe_2O_4$ as compared to Gram positive strain *S.aureus*[27] Fig.(7) and (8) demonstrate that with increasing the $CoFe_2O_4$ concentration, the zone of inhibition also increases. The zone of inhibition was also determined for tetracycline and streptomycin as reference antibiotics. The antibacterial activity of cobalt ferrite NPs is due to their particularly small size which makes a perfect attachment to the membrane of the micro-organism [28-30].

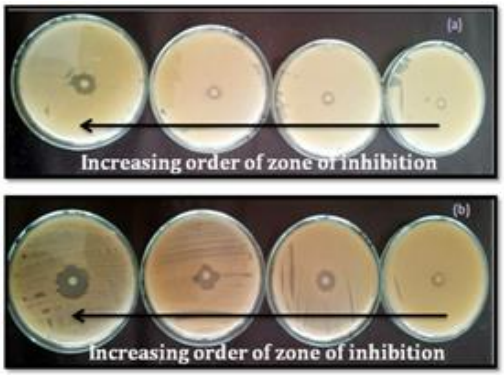

Fig. 7. Zone of inhibition measured for (a) *Staphylococcus aureus* (b) *Escherichia coli* in the presence of different concentrations of $CoFe_2O_4$.

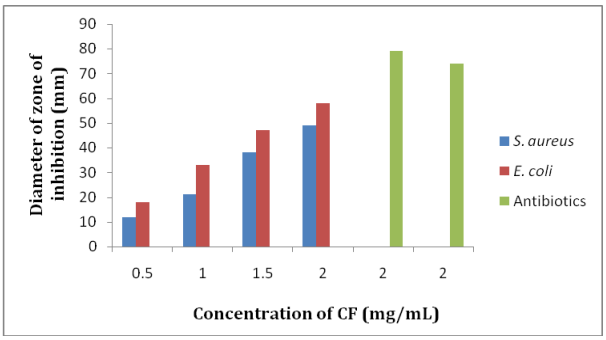

Fig. 8. Comparison of the zone of inhibition as measured in different concentrations of $CoFe_2O_4$ NPs and antibiotics.

The interaction behaviour of cobalt ferrite NPs (product b) with calf-thymus DNA was also investigated. The IR spectral features of pure $CoFe_2O_4$ NPs (product b), pure calf-thymus DNA and $CoFe_2O_4$/calf-thymus DNA nanocomposites are shown in Fig.(9). In Fig.(9a), the spectrum shows an absorption at 585cm^{-1} for the M−O bond of $CoFe_2O_4$[31]. Fig.(9b) presents the characteristics peaks of calf-thymus DNA with the interesting region 1800–700 cm^{-1} describing the deoxyribose stretching of DNA, oscillation of the groups in the heterocyclic nitrogenous bases and stretching vibrations (asymmetric and symmetric) of the phosphate group (PO_2^{-1}). Two feature bands at 1225 and 1085 cm^{-1} depict the asymmetric and symmetric vibrations of PO_2^{-1} respectively [32]. The absorption band at 1054 cm^{-1} appears as a sugar band in the IR spectrum. In Fig.(9c), the spectrum exhibits the presence of a (M−O) bond at 587 cm^{-1} confirming the formation of the CF/calf-thymus DNA nanocomposite. The changes in the intensity ratios of the symmetric and asymmetric vibrations (v_s/v_{as}) of the phosphate group PO_2^{-1} indicate the participation of the PO_2^{-1} group in the synthesis of the bio-nanocomposite [33,34]. The shifting of the guanine (G) band from 1717 to 1708 cm^{-1} and the increase in intensity of the thymine (T) band at 1667 cm^{-1} indicate that the heterocyclic bases are interacting with cobalt ferrite NPs. The shift of the asymmetric and symmetric peaks of the phosphate group (PO_2^{-1}) from 1225 to 1219cm^{-1} and 1085 to 1088cm^{-1} also indicate the interaction of the phosphate group (PO_2^{-1}) with the surface of the ferrites nanoparticles [35]. The interaction of the CF/DNA bio-nanocomposite occurs due to the formation of coordination bonds between cobalt and iron ions on the particle surface and the oxygen atoms in the DNA (phosphate group, O6 in guanine and O4 in thymine) as already explained in the literature [36].

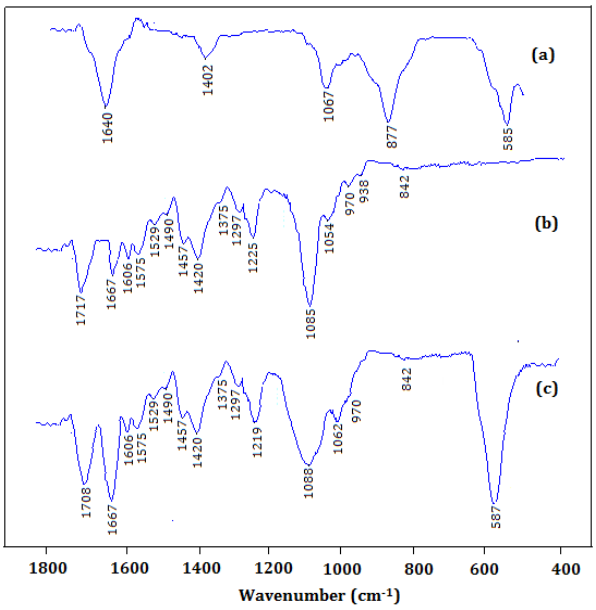

Fig. 9. (a) FT-IR spectra of pure $CoFe_2O_4$ nanopowder (b) Calf-thymus DNA (c) CF/DNA.

CONCLUSIONS

The present study demonstrates the synthesis of cobalt ferrite nanoparticles using a novel surfactant assisted co-precipitation method. The XRD pattern exhibits the presence of a cubic spinel phase in cobalt ferrite NPs. The size of the cobalt ferrite NPs was effectively reduced by applying a surfactant as measured by the XRD pattern which is in agreement with the SEM images. The outstanding magnetic response of cobalt ferrite NPs in the presence of an applied magnetic field may direct them as an efficient nanocarrier for targeted drug delivery. TGA/DSC studies are affirming the presence of a capping agent on the surface of cobalt ferrite NPs. The prepared cobalt ferrite nanoparticles also have an antibacterial potential against E.coli and S.aureus and are capable to develop interactions with nitrogenous bases of DNA. Finally, we can say that the cobalt ferrite NPs prepared by the surfactant assistant method have the potential to be applied as a biomaterial in numerous fields of material engineering, biomedical and biotechnology systems.

REFERENCES

1. O. Yamamoto, *Int. J. Inorg. Mater.*, **3**, 643 (2001).
2. L. Zhang, Y. Jiang, Y. Ding, M. Povey, D. York, *J. Nanopart. Res.*, **9,** 479 (2007).
3. O. Seven, B. Dindar, S. Aydemir, D. Metin, M.A. Ozinel and S. Icli, *J. Photochem. Photobiol. A: Chemistry*, **165**, 103 (2004).
4. R. Brayner, R. Ferrari-Iliou, N. Brivois, S. Djediat, M.F. Benedetti, F. Fiévet, *Nano Lett.*, **6**, 866 (2006).
5. J. Sawai, *J. Microbiol. Methods*, **54,** 177 (2003).

6. X. Meng, H. Li, J. Chen, L. Mei, K. Wang, X. Li, *J. Magn. Magn. Mater*., **321**, 1155 (2009).
7. L. Phua, F. Xu, Y. Ma, C. Ong, *Thin Solid Films*, **517**, 5858 (2009).
8. S. Sun, H. Zeng and D.B. Robinson, *J. Am. Chem. Soc*., **126**, 273 (2004).
9. D.N. Williams, S.H. Ehrman, T.R.P. Holoman, *J. Nanobiotechnol*., **4**, 3, doi:10.1186/1477-3155-4-3 (2006).
10. P. Gong, H. Li, X. He, *Nanotechnology*, **18**, 285604, doi:10.1088/0957-4484/18/28/285604 (2007).
11. M. Banoee, S. Seif, Z.E. Nazari, *J. Biomed. Mater. Res. B: Appl.Biomater*.,**93**, 557 (2010).
12. P. Gajjar, B. Pettee, D.W. Britt, W. Huang, W.P. Johnson, A.J. Anderson, *J. Biol. Engg*., **3**, 1 (2009).
13. R.L. Penn, K. Tanaka, J. Erbs, *J. Cryst. Growth*, **309**, 97 (2007).
14. M. Niederberger, H. Colfen, *Phys. Chem. Chem. Phy*s., **8**, 3271 (2006).
15. K. Nejati and R. Zabihi, *Chem. Cent. J*., **6**, 1 (2012).
16. T.R. Bastami, M.H. Entezari, Q.H. Hu, S.B. Hartono, S.Z. Qiao, *Chem. Eng. J.*, **210**, 157 (2012).
17. Y. Zhang, G.K. Das, R. Xu, T.T.Y. Tan, J. Mater. Chem., **19**, 3696 (2009).
18. R. Mehta, P. Goyal, B. Dasannacharya, R. Upadhyay, V. Aswal, G. Sutariya, *J. Magn. Magn. Mater*., **149**, 47 (1995).
19. O. Ur Rahman, S.C. Mohapatra, S. Ahmad, *Mater. Chem. Phys*., **132**, 196 (2012).
20. S. Kumar, V. Singh, S. Aggarwal, U.K. Mandal and R.K. Kotnala, *J. Phys. Chem. C*, **114**, 6272 (2010).
21. S. Ahmad, U. Riaz, A. Kaushik, *J. Alam, J. Inorg. Organomet. Polym. Mater.*, **19**, 355 (2009).
22. R. Raveendra, P. Prashanth, B. Daruka Prasad, *Int. J. Sci. Res.*,**1**, 543 (2012).
23. G. Allaedini, S.M. Tasirin, P. Aminayi, *Int. Nano Lett*., doi:10.1007/S40089-015-0153-8 (2015).
24. A.C.F. Costa, M.R. Morelli, R.H. Kiminami, *J. Mater. Sci*., **42**, 779 (2007).
25. K. Maaz, S. Karim, A. Mumtaz, S. Hasanain, J. Liu, J. Duan, *J.Magn.Magn.Mater*., **321**, 1838 (2009).
26. N. Sanpo, J. Wang and C.C. Berndt, *J. Nano Res*., **25**, 110 (2013).
27. S.S. Mukhopadhyay, *Nanotechnol. Sci. Appl*., **7,** 63 (2014).
28. L.L. Radke, B.L. Hahn, D.K. Wagner, P.G. Sohnle, Clin. Immun. Immunopathol., **73**, 344 (1994).
29. R.M. Wang, B.Y. Wang, Y.F. He, W.H. Lv, J.F. Wang, *Polym. Advan. Technol*., **21**, 331 (2010).
30. A. Baykal, N. Kasapoglu, Y. Koseoglu, A. C. Basaran, H. Kavas, M.S. Toprak, *Cent. Eur. J. Chem*., **6**, 125 (2008).
31. D.K. Jangir, G. Tyagi, R. Mehrotra, S. Kundu, *J. Mol. Struct.*, **969**, 126 (2010).
32. H. Tajmir-Riahi, R. Ahmad, M. Naoui, S. Diamantoglou, *Biopolymers*, **35**, 493 (1995).
33. A.U. Metzger, T. Schindler, D. Willbold, *FEBS lett*., **384**, 255 (1996).
34. H. Malonga, J. Neault, H. Arakawa, H. Tajmir-Riahi, *DNA Cell Biol*., **25**, 63 (2006).
35. J. Anastassopoulou, J. Mol. Struct., 651,19 (2003).
36. K. Maaz, A. Mumtaz, S. Hasanain, A. Ceylan, *J. Magn. Magn. Mater*., **308**, 289 (2007).

СИНТЕЗА, СТРУКТУРНИ И БИОЛОГИЧНИ ИЗСЛЕДВАНИЯ НА НАНОЧАСТИЦИ ОТ КОБАЛТОВИ ФЕРИТИ

М.У. Мущак[1], М. Имран[1], С. Башир[2], Ф. Канвал[1], Л. Миту[3*]

[1]*Институт по химия, Университет в Пунджаб, Лахор-54890, Пакистан*
[2]*Департамент по физика, Научен факултет, Университет в Малая-50603, Куала Лумпур, Малайзия*
[3]*Департамент по химия, Университет в Питещ, Питещ-110040, Румъния*

Постъпила на 31 май 2015 г.; приета на 16 декември 2015 г.

(Резюме)

Синтезирани са наночастици от кобалтови ферити, $CoFe_2O_4$ (CF) по метода на съутаяване с използването на нов мономерен сърфактант (сорбитол). За охарактеризирането им са използвани Фуриерова инфрачервена спектроскопия (FTIR), прахов рентгеноструктурен анализ (XRD), магнетометър с вибрираща проба. Потвърдено е наличието на (M–O) - връзка по абсорбционната линия при 589 cm^{-1} в FTIR-спектъра. VSM-изследвания разкриват свръх-парамагнитни свойства на наночастиците от кобалтови ферити, имащи наситена магнетизация съответно 62.55 emu/g и 59.89 emu/g за кобалтовите ферити, приготвени без и със сърфактант. Хистерезисните контури показват пренебрежим хистерезис, остатъчен магнетизъм и коерцитивност при 300 K. Рентгеноструктурният анализ (XRD) потвърждава като единствена фаза шпинелна кубична структура. Електронно-микроскопски (SEM) микрографии са използвани за определянето на размерите на частиците като 28 nm с използването на сърфактант и 60 nm без сърфактант. Микрографиите са използвани и за анализ на разпределението по размери. Съдържанието на сърфактант е изследвано чрез термогравиметрични измервания. Направен е скрийнинг на приготвените частици за антибактериална активност срещу *Escherichia coli* and *Staphylococcus aureus*, който показва значителна активност. Освен това е изследвано взаимодействието на наночастиците с ДНК от телешки тимус.